

56 GBaud O-Band Transmission using a Photonic BiCMOS Coherent Receiver

Pascal M. Seiler^(1,2), Anna Peczek⁽³⁾, Georg Winzer⁽²⁾, Karsten Voigt^(1,2),
Stefan Lischke⁽²⁾, Adel Fatemi⁽²⁾, Lars Zimmermann^(1,2)

⁽¹⁾ Technische Universität Berlin, Institut für HF- und HL-Systemtechnologien, Einsteinufer 25, 10587 Berlin, Germany, seiler@tu-berlin.de

⁽²⁾ IHP GmbH, Im Technologiepark 25, 15236 Frankfurt (Oder), Germany

⁽³⁾ IHP Solutions GmbH, Im Technologiepark 25, 15236 Frankfurt (Oder), Germany

Abstract We present a photonic BiCMOS coherent receiver dedicated to the O-band and achieve detection at up to 56 GBd using quadrature-phase shift-keying (QPSK) at various optical signal-to-noise ratios (OSNRs). Transmission experiments are performed and potential applications within that power budget are discussed.

Introduction

The importance and immense growth of large-scale data centers (DC) has been a driving factor for modern optical communication for the last years, and will continue to be one in the future. There is increasing demand of intra-DC interconnects up to a few km, which are presently served by direct-detection (DD) schemes operating in the O-band (1260 nm to 1360 nm). To support future data rates of > 1 Tb/s, a flexible, and scalable technology is required. Given the already well established O-band for these link distances, the deployment of coherent transceivers dedicated to the O-band is an attractive option. However, that leads to some key differences between C- and O-band coherent communication links: (1) standard single-mode fibers (SMF) exhibit a chromatic dispersion minimum around 1310 nm and (2) a nearly twice as large attenuation than at 1550 nm. (3) The polarization-mode dispersion (PMD) is significantly reduced in comparison to long-haul communication. (4) While the use of optical amplifiers within the C-band is acceptable for long-haul communication, their deployment in the O-band becomes unfeasible, given the stringent power restriction set by DD schemes, which are the present data links of choice in that domain. Both points (1) and (3) lead to a potentially reduced digital signal processing (DSP), which in turn reduces the power consumption. This is further enhanced by (4) and the intrinsic scalability of coherent data links towards higher bit rates using higher order modulation formats. While there has been extensive research towards silicon-based integrated coherent receivers within the C-band^{[1]–[9]}, there has been little research on silicon-based receivers and their potential per-

formance benefits within the O-band^[10], especially considering the power restrictions set by the omission of optical amplification and the increased losses of SMF within that band. In this work, we present an O-band monolithic single-polarization coherent receiver, fabricated in IHP's 0.25 μm photonic BiCMOS technology^[11], and demonstrate its performance at 56 GBd transmission experiments. We furthermore evaluate potential applications for intra-DC applications at data rates > 1 Tbit/s based on the determined power budgets. To the best of our knowledge, this is the first performance evaluation of a monolithic silicon-based coherent O-band receiver in a fiber transmission. All receiver components are fabricated on the same wafer.

Device Characterization

The schematic of the integrated coherent receiver is shown in Fig. 1, with a photograph of the fabricated structure in the top inset. For the electrical circuit, only the part for the quadrature (Q) component is shown, while the circuit for the in-phase (I) component is omitted. Optical coupling is performed by a fiber array and 1D grating couplers. The 90° hybrid is achieved by a 4 x 4 multi-mode interference coupler (MMI). The simulated imbalance and phase error remains within 3.3 dB and 6.9° over the full O-band, respectively. The electrical section consists of an input stage, two variable gain amplifiers (VGAs) and a 50 Ω output buffer. The VGAs support an automatic gain control, which is used throughout this work. The receiver supplies differential outputs for the I - and Q-component, respectively. Further information on the electrical section of the receiver can be found in Ref.^[12]. Input stage and

©2020 IEEE. Personal use of this material is permitted. Permission from IEEE must be obtained for all other uses, in any current or future media, including reprinting/republishing this material for advertising or promotional purposes, creating new collective works, for resale or redistribution to servers or lists, or reuse of any copyrighted component of this work in other works.

This work was supported by the H2020-SPACE-ORIONAS project from the European Union's Horizon 2020 research and innovation program under grant agreement No. 822002. This is an own version of manuscript submitted to IEEE for publication. Posting of own manuscript version is permitted under IEEE sharing policies: <https://www.ieee.org/publications/rights/index.html>

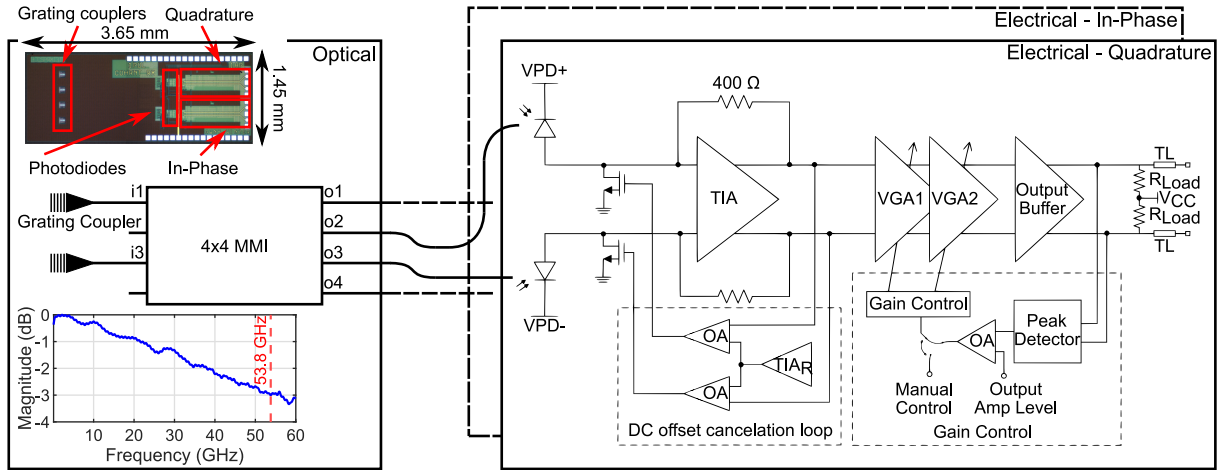


Fig. 1: Schematic of the integrated coherent receiver, separated in optical and electrical parts. The second analogous circuit for the in-phase component is omitted. The top inset shows a photograph of the fabricated receiver, and the bottom inset the small-signal response of an exemplary photodiode. OA: operational amplifier, TIA: transimpedance amplifier, TIA_R: Replica TIA, VGA: variable gain amplifier, TL: transmission line, MMI: multi-mode interference coupler, VPD: photodiode bias voltage.

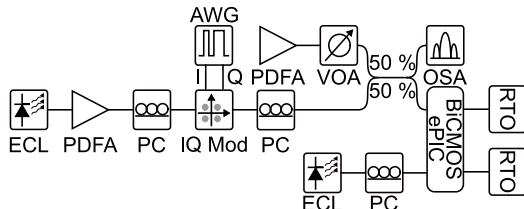
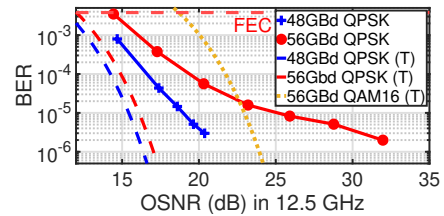


Fig. 2: Heterodyne measurement setup with integrated O-band coherent receiver. A QPSK is applied using a commercial C-band IQ-modulator (IQ Mod). AWG: arbitrary waveform generator, PC: polarization controller, OSA: optical spectrum analyzer, PDFA: praseodymium-doped fiber amplifier, VOA: variable optical attenuator.

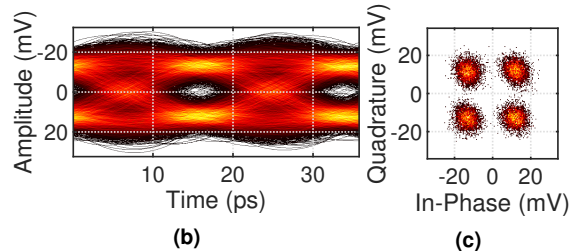
VGAs are supplied with 2.4 V and 3.6 V, respectively. The total power consumption and size of the integrated coherent receiver is 485 mW and 3.65 mm x 1.45 mm, respectively. Due to the necessity of an LO for proper electrical behavior, the opto-electrical bandwidth cannot be measured using traditional lightwave component analyzers (LCA). In the absence of a properly calibrated system, an exemplary photodiode bandwidth of a process control structure of the same wafer is given in the bottom inset of Fig. 1. The bandwidth is measured using a calibrated LCA (Agilent N4373D) and the 3 dB bandwidth is approximately 54 GHz. The electrical circuit can be expected to have a bandwidth of >33 GHz^[12].

Back-to-Back Experiment

Fig. 2 shows the heterodyne measurement setup used for the back-to-back (B2B) experiment. Both O-band lasers used for signal and local oscillator (LO) are external cavity lasers (ECL, Keysight 81606A and 81600B), set to 1310 nm. The signal laser is pre-amplified to +16 dBm (which is within the available fiber coupled output power for lasers available at that wavelength^[13]) using a praseodymium-doped fiber amplifier (PDFA,



(a)



(b)

(c)

Fig. 3: (a) BER vs. OSNR for 48 GBd and 56 GBd QPSK. The (T) in the legend denotes the theoretical limit. The FEC-limit is set at $3.8 \cdot 10^{-3}$. (b) Recovered eye diagram and (c) constellation of 50 k samples at 56 GBd at an OSNR of 14.5 dB. The eye diagram has been interpolated.

FiberLabs AMP-FL8611-OB). The use of a C-band IQ modulator (IQ Mod, ID Photonics OMFT, specified operating range 1525 nm - 1570 nm) is given the only recently emerged interest in coherent transmissions in the O-band and therefore the lack of commercially available, dedicated modulators. While the modulator exhibits around 3 dB increased losses within the O-band, the increase of imbalance at 1310 nm is unknown. The performance is closely monitored using an optical spectrum analyzer (OSA, Advantest Q8384, resolution bandwidth 0.01 nm) throughout the measurement. The electrical 550 mV_{PP} PRBS15 patterns for the modulator are supplied using an arbitrary waveform generator (AWG, Keysight M8194A). The modulation format is quadrature-phase shift-keying (QPSK) at baud rates up to 56 GBd, with

root raised cosine pulse shaping at a roll-off factor of 0.3. Following, the modulated signal is connected to a 3 dB coupler for noise loading and monitoring using the OSA. For noise loading, a second PDFA (FiberLabs AMP-FL5601-OB) and a variable optical attenuator (VOA, Keysight N7752A) are used. The resulting power at the coherent receiver for the signal and LO are -3.6 dBm and +12 dBm, respectively. The optical- and electrical contacting is achieved on-wafer at a stable temperature of 28 °. While the receiver supplies differential outputs for I and Q, only single-ended signals are connected to the real-time oscilloscopes (RTO, Tektronix DPO77002SX, sampling rate 200 GSa/s) 70 GHz channels. The RTO bandwidth has been intentionally limited to 50 GHz due to the beating between signal and LO being below 1 GHz. DC-terminated bias-tees are used for DC blocking. The recorded data is analyzed using Tektronix optical modulation analysis software (OM1106), and includes FIR-filtering based on the pulse-shaping, phase recovery, and equalization by applying a constant modulus algorithm. The determined bit-error rate (BER) for varied optical signal-to-noise ratios (OSNRs) is given in Fig. 3a, with the dashed lines showing the respective theoretical limit^{[14],[15]}. The reference bandwidth for the OSNR is 12.5 GHz, which is 71.6 pm optical bandwidth at 1310 nm. The OSNR is varied between approx. 32 dB and 14 dB, and the respective BER are measured (within the statistical limit of up to 10^7 bits for error rates below 10^{-6}). Operation below the forward error-correction (FEC) limit is found at OSNRs of 14.7 and 14.5 dB for 48 and 56 GBd, respectively. An example of the recovered eye diagram and constellation for 56 GBd at an OSNR of 14.5 dB and color-coded to a logarithmic scale can be found in Fig. 3b and 3c. The eye diagram has been interpolated.

Transmission Experiment

A VOA and various SMF spools are added subsequent to the IQ modulator and the noise loading in Fig. 2 is turned off. For each fiber length, the launch power is varied and the BER is determined analogously to the B2B experiment. No compensation for chromatic dispersion is added to the post-processing. The measured BERs at 56 GBd are given in Fig. 4. The power margins for 4 km, 8.5 km, and 13 km link distance for an operation below the FEC-limit are 7 dB, 5.3 dB, and 3.8 dB, respectively. While limited in the available

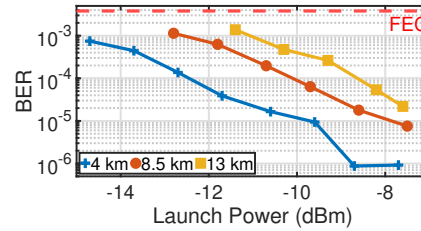


Fig. 4: BER vs. launch power for 56 GBd at different transmission distances. The FEC-limit is set at $3.8 \cdot 10^{-3}$.

span length, the results shown in Fig. 4 indicate a sufficient performance below the FEC-limit even for higher link distances. Alternatively, the available budget would allow for a higher order modulation format like QAM16 for the targeted link distances of a few km, since the theoretical penalty by transitioning from QPSK to QAM16 is approximately 7 dB (comp. Fig. 3a). While receiver properties like linearity become increasingly important for this, the study of QAM16 is presently obstructed by the unavailability of dedicated modulators.

Conclusions

Future high-speed intra-DC interconnects will have to enable rapidly increasing data rates, even at shorter link distances. In this work, we presented a monolithically integrated photonic BiCMOS coherent receiver, operating at 1310 nm. The presented power budget at the targeted distances of around 4 km is approximately 8 dB using QPSK. Which, even with the impairments of a C-band modulator, would theoretically allow for higher formats like QAM16. In a potential application, that could enable a transmission of 200 GBd (400 GBd using dual polarization) and thus up to 1.6 Tb/s when 4 channels are utilized, which is compatible to reported silicon photonic O-band IQ modulators^[16]. Estimation of overall power budget of O-band coherent DC interconnects requires in depth analysis of short link DSP (estimated to be 3-4 W per channel^[17]), which should be studied as the next step.

Acknowledgements

The authors would like to thank Keysight Technologies for supplying the AWG. This work was supported in part by the German Research Foundation (DFG) through the projects EPIC-Sense (ZI 1283-6-1) and EPIDAC (ZI 1283-7-1), by the Federal Ministry of Education and Research (BMBF) through project PEARLS (13N14932), and the European Commission through project H2020-SPACE-ORIONAS (822002).

References

- [1] C. R. Doerr *et al.*, "Monolithic silicon coherent receiver", in *Opt. Fiber Commun. Conf. (OFC)*, Mar. 2009, pp. 1–3.
- [2] M. Kroh *et al.*, "Hybrid integrated 40 Gb/s DPSK receiver on SOI", in *Opt. Fiber Commun. Conf. (OFC)*, Mar. 2009, pp. 1–3.
- [3] C. R. Doerr *et al.*, "Packaged monolithic silicon 112-Gb/s coherent receiver", *IEEE Photon. Technol. Lett.*, vol. 23, no. 12, pp. 762–764, 2011.
- [4] C. Doerr *et al.*, "Single-chip silicon photonics 100-Gb/s coherent transceiver", in *Opt. Fiber Commun. Conf. (OFC)*, Mar. 2014, pp. 1–3.
- [5] P. Dong *et al.*, "Monolithic silicon photonic integrated circuits for compact 100⁺ Gb/s coherent optical receivers and transmitters", *IEEE J. Sel. Topics Quantum Electron.*, vol. 20, no. 4, pp. 150–157, Jan. 2014.
- [6] G. Winzer *et al.*, "Monolithic photonic-electronic QPSK receiver for 28Gbaud", in *Opt. Fiber Commun. Conf. (OFC)*, Mar. 2015, pp. 1–3.
- [7] J. Verbist *et al.*, "A 40-GBd QPSK/16-QAM integrated silicon coherent receiver", *IEEE Photon. Technol. Lett.*, vol. 28, no. 19, pp. 2070–2073, Jun. 2016.
- [8] J. Zhang *et al.*, "Compact low-power-consumption 28-Gbaud QPSK/16-QAM integrated silicon photonic/electronic coherent receiver", *IEEE Photon. J.*, vol. 8, no. 1, pp. 1–10, 2016.
- [9] S. Gudyriev *et al.*, "Coherent ePIC receiver for 64 GBaud QPSK in 0.25 μ m photonic BiCMOS technology", *J. Lightw. Technol.*, vol. 37, no. 1, pp. 103–109, 2019.
- [10] C. Doerr *et al.*, "O, E, S, C, and L band silicon photonics coherent modulator/receiver", in *Opt. Fiber Commun. Conf. (OFC)*, Mar. 2016, pp. 1–3.
- [11] D. Knoll *et al.*, "High-performance photonic BiCMOS process for the fabrication of high-bandwidth electronic-photonic integrated circuits", in *IEEE Int. Electron Devices Meeting (IEDM)*, Dec. 2015, pp. 15.6.1–15.6.4.
- [12] A. Awmy *et al.*, "A linear differential transimpedance amplifier for 100-Gb/s integrated coherent optical fiber receivers", *IEEE Trans. Microw. Theory Techn.*, vol. 66, no. 2, pp. 973–986, Sep. 2018. DOI: 10.1109/TMTT.2017.2752170.
- [13] P. Doussiere *et al.*, "Very high-power 1310nm InP single mode distributed feed back laser diode with reduced linewidth", in *Novel In-Plane Semiconductor Lasers VI*, C. Mermelstein and D. P. Bour, Eds., International Society for Optics and Photonics, vol. 6485, SPIE, 2007, pp. 129–136. DOI: 10.1117/12.701321.
- [14] R. Essiambre *et al.*, "Capacity limits of optical fiber networks", *J. Lightw. Technol.*, vol. 28, no. 4, pp. 662–701, 2010.
- [15] J. G. Proakis and M. Salehi, in *Digital communications, 5th ed.*, McGraw-Hill Higher Education, 2008.
- [16] A. Samani *et al.*, "180 Gb/s single carrier single polarization 16-QAM transmission using an O-band silicon photonic IQM", *Opt. Express*, vol. 27, no. 10, pp. 14447–14456,
- [17] J. Cheng *et al.*, "Power consumption evaluation of ASIC for short-reach optical interconnects", in *2018 23rd Opto-Electronics and Communications Conference (OECC)*, 2018, pp. 1–2.